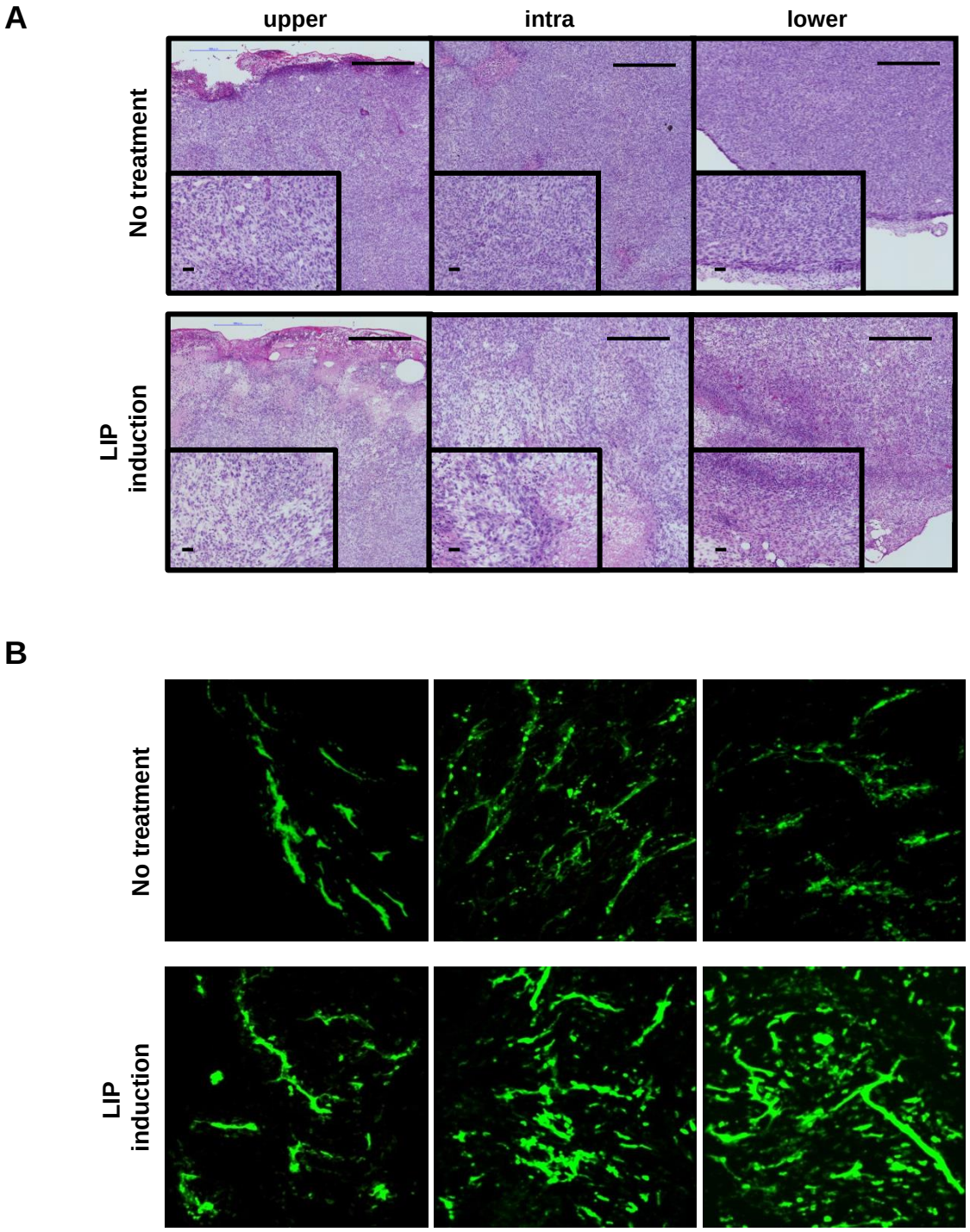

Supplemental figure S1.
Histological analysis and angiogenesis of tumor tissue during tumor regression, accompanied by LIP.
A. Frozen sections of tumor tissue were fixed, and histological analysis was by H&E staining. Each panel indicates upper (left panel), intra (middle panel), and lower (right panel) part of tumor tissue 15 days after LIP induction. Photographs show representative data from 2 independent experiments with n=3. Scale bar: main figures, 500μm; insets, 50μm. **B.** During tumor regression, tumor angiogenesis in LIP-induced hosts was comparable to that in no-treatment hosts. Tumor tissues were harvested on day 14 after LIP induction, and tissue sections (50μm) that had been stained with FITC-conjugated TOMATO-lectin (green) and perfused were observed under confocal laser scanning microscopy. Figures show 3 distinct fields of tumor tissue from 3 mice in 2 independent experiments.

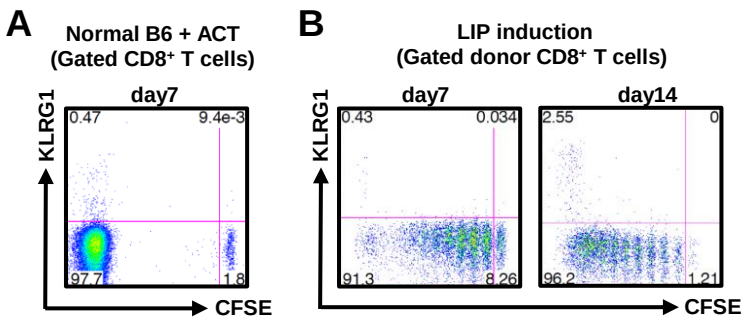

Supplemental figure S2.

KLRG1^{+} CD8^{+} T cells do not accumulate during LIP in tumor-free hosts.

Ly5.1/5.2 C57BL/6 mice were sub-lethally irradiated to induce lymphopenia, and then injected with CFSE-labeled CD44^{low} Ly5.1^{+} CD8^{+} T cells. On days 7 and 14, CFSE decay and KLRG1 expression of donor (Ly5.2^{-}) CD8^{+} T cells were assessed by 8-color FACS (**B**). For the control, non-irradiated mice were injected with CFSE-labeled donor cells (**A**).

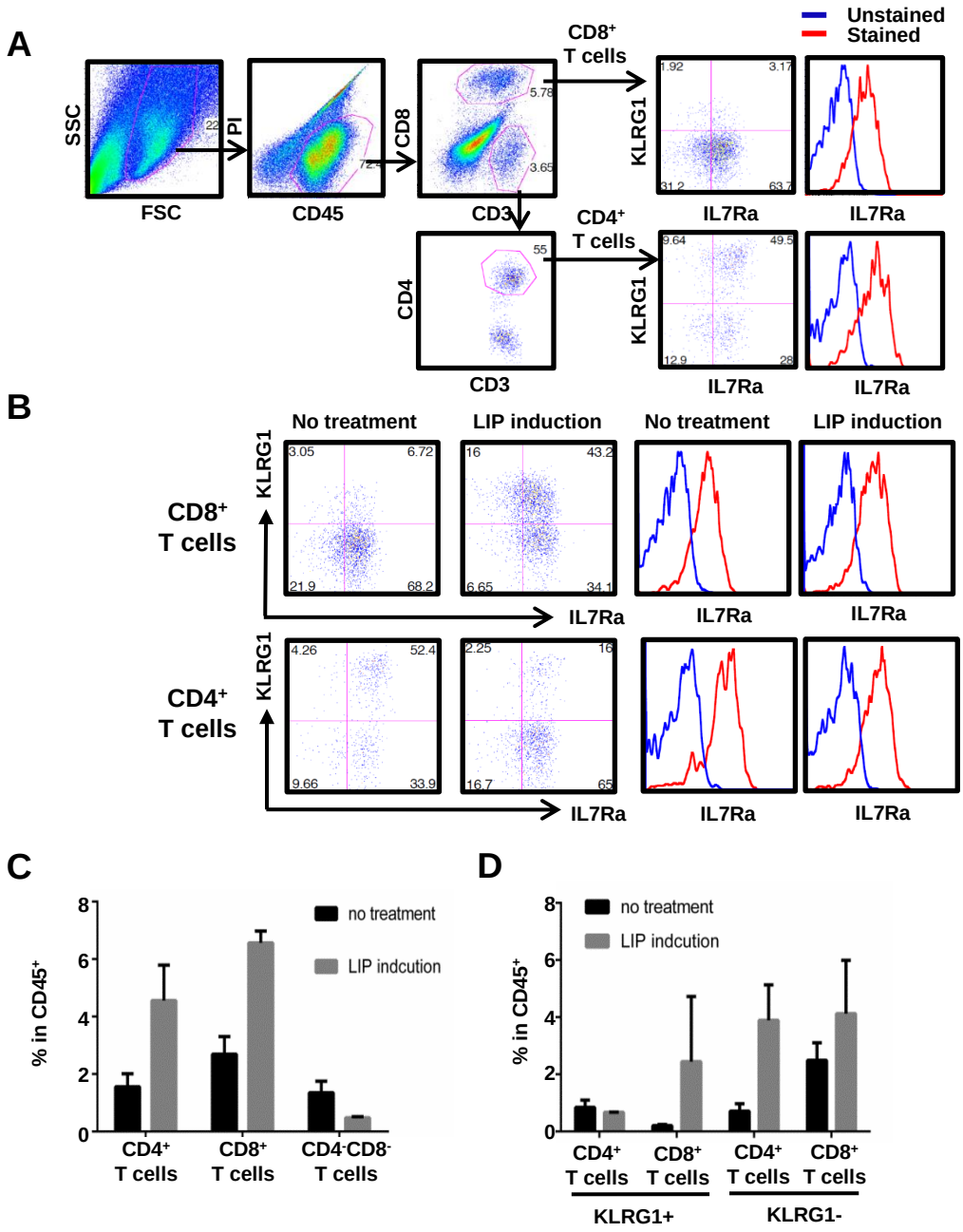

Supplemental figure S3.

LIP induction led to the accumulation of KLRG1-positive CD8⁺ T cells and KLRG1-negative CD4⁺ T cells in tumor tissue which expressing IL7Rα.

The experimental procedure is as for Fig. 1. **A.** Gating strategy for flow cytometry analysis of TILs. Cells were first gated for singlet and CD45⁺ lymphocytes. The lymphocyte population was then gated based upon the expression of CD3 and CD8a to determine CD8⁺ T cells. The CD3⁺CD8⁻ population was further analyzed for CD4 expression to identify CD4⁺ T cells. **B.** TILs maintained IL7 receptor expression. **C.** CD8⁺ and CD4⁺ T cells accumulated in tumor tissue, accompanied by LIP. Bars, SD based on results from 3 mice in one of 3 experiments. The infiltration of CD8⁺ and CD4⁺ T cells was also quantified by FACS and IHC (Fig. 1). **D.** KLRG1⁻ CD4⁺ T cells and KLRG1⁺ CD8⁺ T cells accumulated in the tumor during LIP. The graph shows the quantification of KLRG1⁺ and KLRG1⁻ T cells in TILs. Bars, SD based on the results obtained from 3 mice in one of 3 experiments.

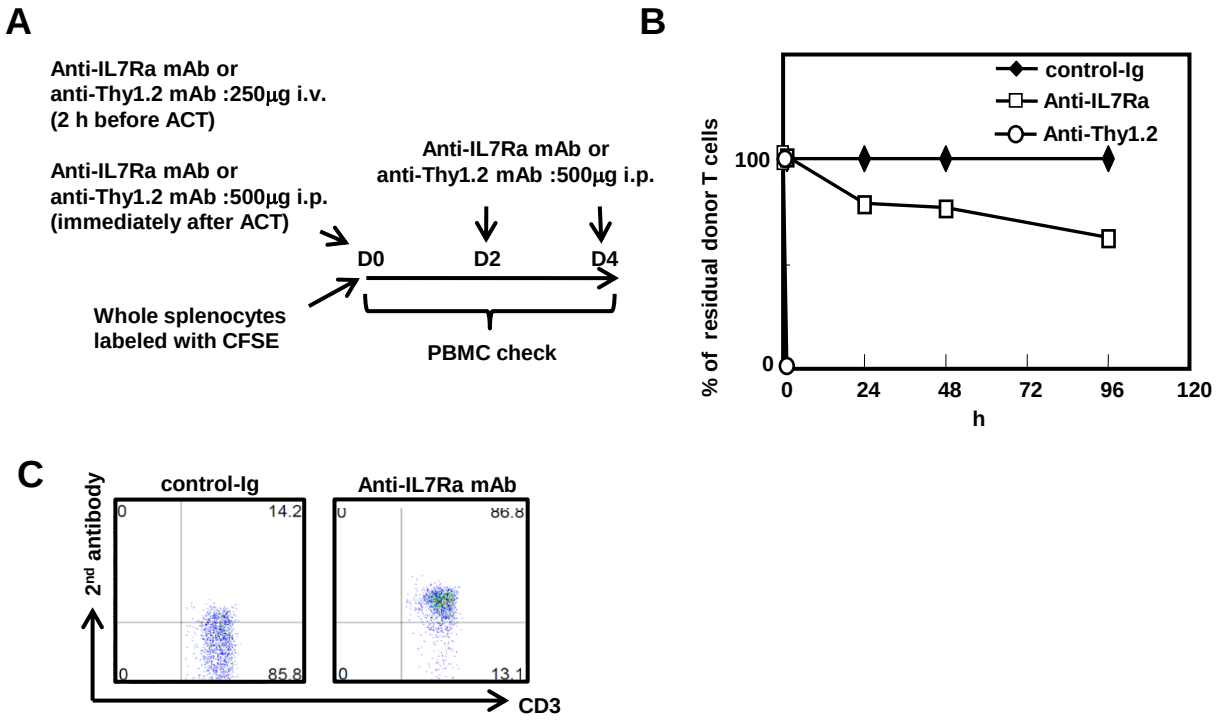

Supplemental figure S4.

Blocking IL7R signaling does not deplete donor T cells by opsonization.

A. Experimental protocol for *in vivo* depletion assay. CFSE-labeled syngeneic splenocytes were transferred into normal mice. Mice received 500μg/day of either control-Ig, anti-IL7Ra mAb (A7R34), or anti-Thy1.2 mAb (30H12) every other day from day 0 to 4. At 1, 24, 48, and 96 h after transfer, the percentage of donor T cells remaining in PBMCs were assessed by FACS, using $CFSE^+$ $B220^+$ cells ($IL7Ra^-$ $Thy1.2^-$) as internal controls. **B.** Kinetics of donor T cells in mice treated with anti-IL7Ra mAb. Control-Ig, black diamonds (◆); anti-IL7Ra mAb, white squares (□); anti-Thy1.2 mAb, white circles (○). **C.** Demonstration that anti-IL7Ra mAb becomes bound to donor $CD3^+$ cells. Cells were harvested from spleen 120 h after transfer, then stained with FITC-conjugated secondary antibody (anti-rat IgG) to detect the binding of anti-IL7Ra mAb on the residual donor ($CFSE^+CD3^+$) T cells.

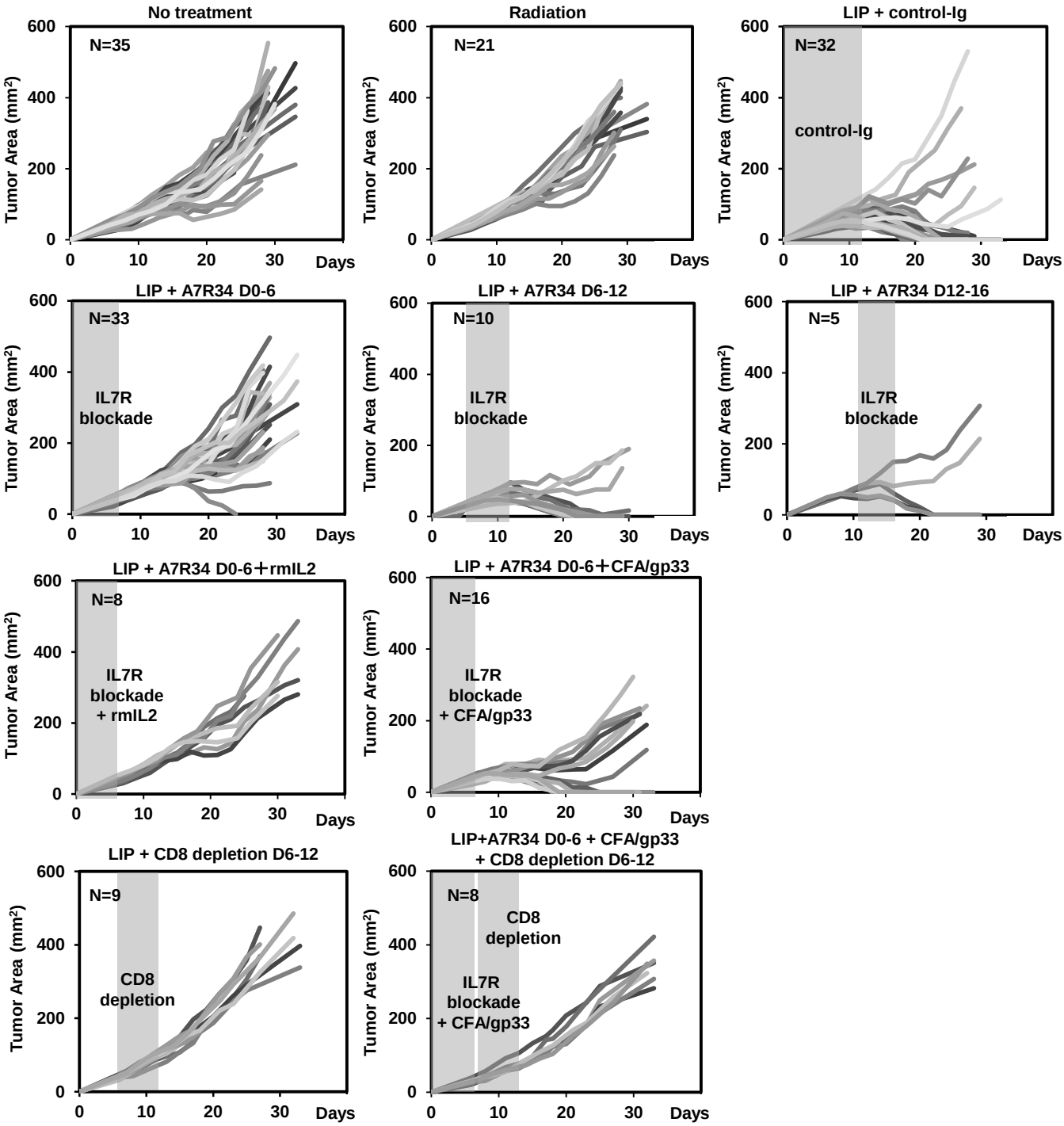

Supplemental figure S5.

Tumor growth in individual mice

Each line represents tumor growth in one mouse. Total number of mice in each experimental group is indicated in the each graph (e.g. No treatment group: n=35). The percentage of mice with tumor rejection and the statistical significance between no-treatment *vs* other treatment groups are indicated in Table 1.

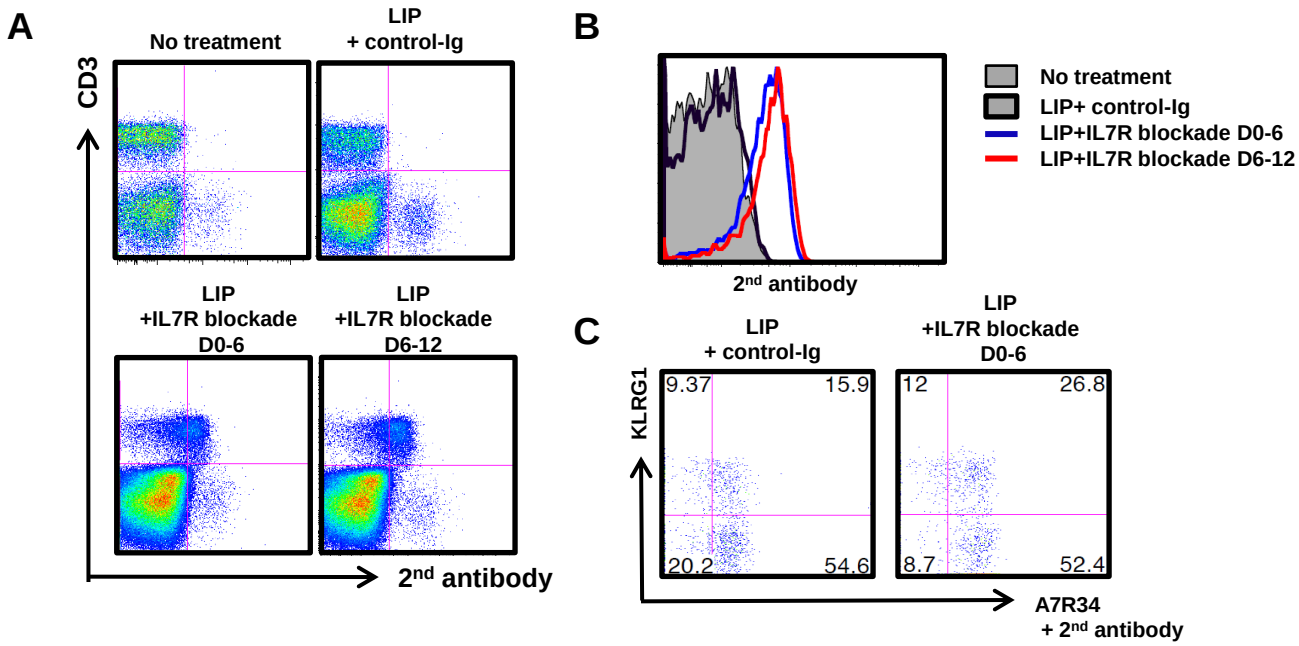

Supplemental figure S6.

Effector CD8$^+$ T cells maintain IL7Rα expression during LIP. Anti-IL7Ra mAb binds to T cells, but does not induce the down-regulation of IL7Rα expression.

A and B. Binding of anti-IL7Ra mAb on T cells (A) and CD8$^+$ T cells (B) 15 days after LIP induction. Splenocytes were recovered from mice treated with LIP induction and administration of control-Ig or anti-IL7Ra mAb, and the binding of anti-IL7Ra mAb on cell surfaces was detected by staining with FITC-conjugated secondary antibody. Histograms show the expression of IL7Ra on CD8$^+$ T cells. No treatment; gray filling, LIP induction and control-Ig treatment; black line, IL7R blockade D0-6; blue line, IL7R blockade D6-12 red line. **C.** KLRG1$^+$ effector CD8$^+$ T cells maintained IL7Rα expression in the presence or absence of IL7R blockade. Experimental procedure is similar to that described in Fig. 3. To confirm the expression of IL7Rα on CD8$^+$ T cells, PBMCs were first stained with purified anti-IL7Ra mAb, and then IL7Rα expression was assessed by FITC-conjugated secondary antibody staining. Dot plots indicate representative data at 24 days after LIP treatment in one of two independent experiments with n=3.

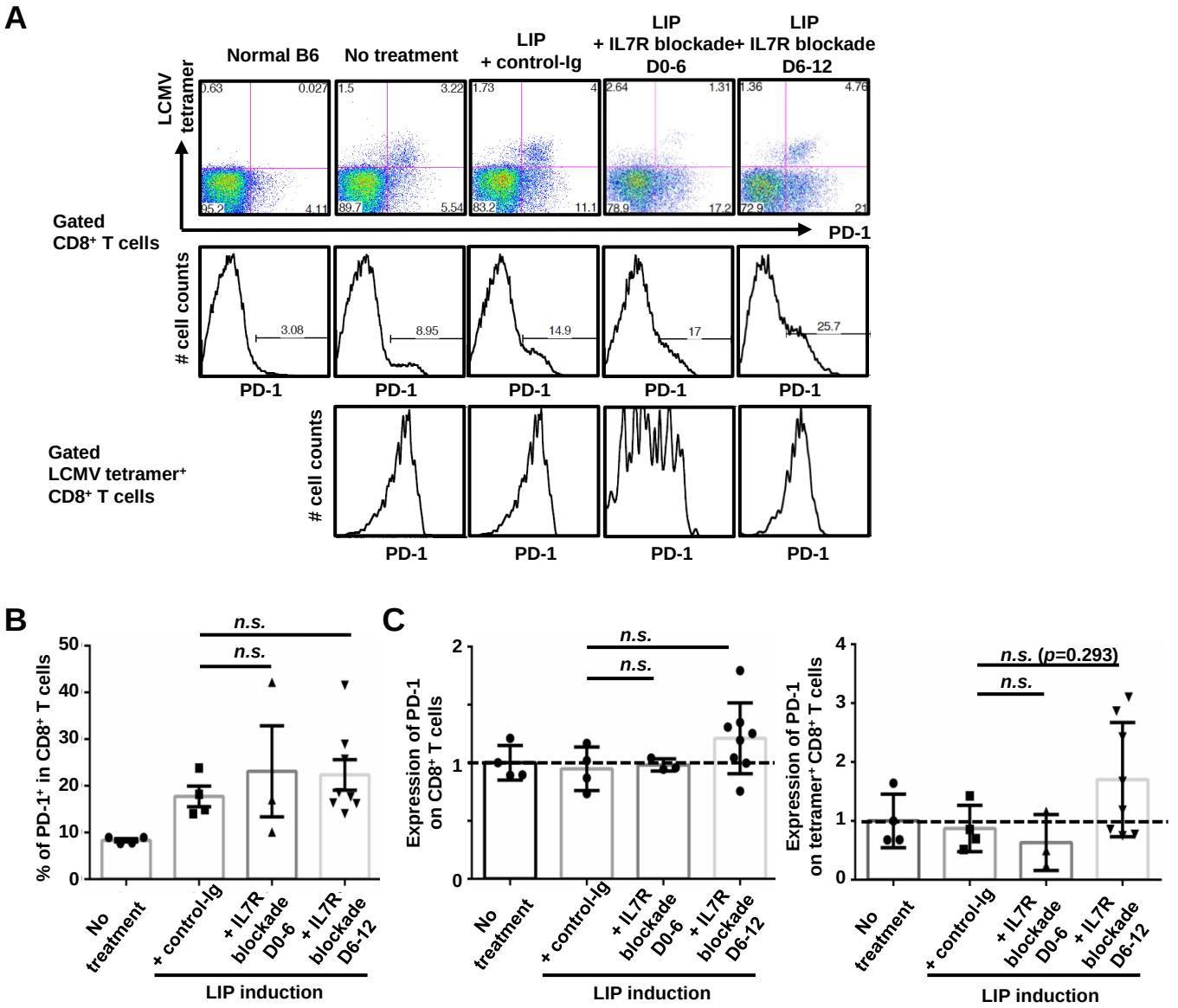

Supplemental figure S7.

PD-1 expression was not altered by IL7R blockade under LIP induction of tumor bearing hosts.

A. Percentage of PD-1$^+$ cells in CD8$^+$ T cells were not changed by IL7R blockade. Experimental procedure as described in Fig 5. Histograms and dot plots show data from two independent experiments with n=3 or 5. **B.** The percentage of PD-1$^+$ cells in CD8$^+$ T cells. **C.** PD-1 expression on LCMV tetramer$^+$ CD8$^+$ T cells. The geometric mean of PD-1$^+$ on CD8$^+$ T cells (left graph) or LCMV tetramer$^+$ CD8$^+$ T cells (right graph) normalized against the no-treatment group. Bars, SE based on results of 4 mice (no-treatment and LIP+control-Ig), 3 mice (LIP+IL7R blockade D0-6), and 8 mice (LIP+IL7R blockade D6-12), respectively, from two repeated experiments.

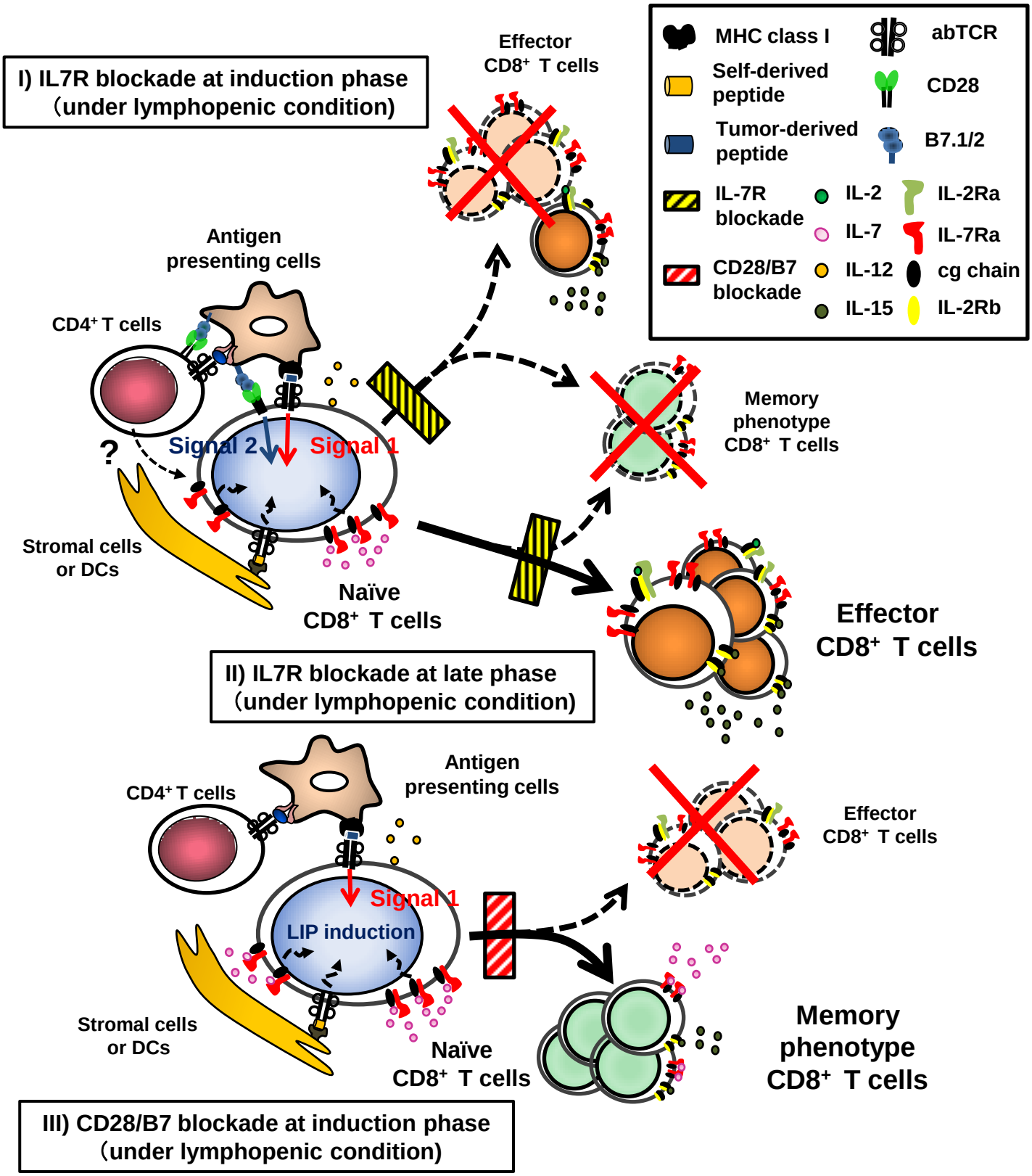

Supplemental figure S8.

Induction of effector CD8+ T cells against TAAs depends on initial expansion through LIP and functional differentiation following CD28 signaling.

In lymphopenic hosts, LIP of naïve T cells is driven by TCR signaling via self-peptide/MHC complexes and IL7R signaling. With IL7R blockade at the induction phase, LIP of naïve T cells is inhibited, resulting in reduced expansion of effector CD8+ T cells which recognize TAAs (Scheme I). With later IL7R blockade (around day 6), the activation of effector CD8+ T cells is dissociated from LIP. In contrast, LIP of naïve T cells depends on certain IL7R signals (Scheme II). A CD28 signal is essential for the functional differentiation of effector CD8+ T cells during LIP. If the CD28 signal is defective during LIP, effector differentiation is inhibited, but LIP of naïve T cells occurs, and naïve CD8+ T cells acquire a memory phenotype (Scheme III).